Hindawi Publishing Corporation
EURASIP Journal on Wireless Communications and Networking
Volume 2010, Article ID 945765, 15 pages
doi:10.1155/2010/945765

Research Article

Parity-Check Network Coding for Multiple Access Relay Channel in Wireless Sensor Cooperative Communications

Bing Du and Jun Zhang

School of Electronics and Information Engineering, Beijing University of Aeronautics and Astronautics, Beijing 100191, China

Correspondence should be addressed to Bing Du, ice.dudu@yahoo.com.cn

Received 27 September 2009; Revised 30 December 2009; Accepted 12 April 2010

Academic Editor: Zhi-Hong Mao

Copyright © 2010 B. Du and J. Zhang. This is an open access article distributed under the Creative Commons Attribution License, which permits unrestricted use, distribution, and reproduction in any medium, provided the original work is properly cited.

A recently developed theory suggests that network coding is a generalization of source coding and channel coding and thus yields a significant performance improvement in terms of throughput and spatial diversity. This paper proposes a cooperative design of a parity-check network coding scheme in the context of a two-source multiple access relay channel (MARC) model, a common compact model in hierarchical wireless sensor networks (WSNs). The scheme uses Low-Density Parity-Check (LDPC) as the surrogate to build up a layered structure which encapsulates the multiple constituent LDPC codes in the source and relay nodes. Specifically, the relay node decodes the messages from two sources, which are used to generate extra parity-check bits by a random network coding procedure to fill up the rate gap between Source-Relay and Source-Destination transmissions. Then, we derived the key algebraic relationships among multidimensional LDPC constituent codes as one of the constraints for code profile optimization. These extra check bits are sent to the destination to realize a cooperative diversity as well as to approach MARC *decode-and-forward* (DF) capacity.

1. Introduction

The demand for ubiquitous communications has motivated the deployment of a variety of wireless devices and technologies that accommodate ad hoc communications. In large numbers, such devices, despite their different sizes, processing constraints, and levels of affordability, form a Wireless Sensor Network (WSN). The WSN cooperatively monitors the physical world and enables sharing of computing capabilities, bandwidth, and energy resources, offering more integrated and essential information than with any single-sensor node. The WSN is generally built as a hierarchical structure by placing a sparse network of access points connected by a high-bandwidth network within a random homogeneous ad hoc network, in which wireless relay nodes serve exclusively as forwarders [1], as in Figure 1. In addition, the hierarchical sensor network with an access point and a single forwarding node can be modeled as a Multiple Access Relay Channel (MARC), which is a multisource extension of the well-known single-user relay channel [2]. With dedicated relay nodes, cooperative communications [3–7] among WSN exploit the broadcast characteristics and inherent spatial diversity to form a large transmit and/or receive antenna array (also known as Multiple Input Multiple Output, MIMO). Collaborative clusters are able to achieve spatial diversity as well as rate multiplexing by making "negotiations" among neighboring nodes to fully utilize the rich wireless propagation environments across multiple protocol layers and offers numerous opportunities to improve network performance in terms of throughput [2], reliability [8–10], longevity, and flexibility.

The most important element in cooperative communications is coding protocols responsible for interaction between cooperative nodes. Over the past few years, several coding strategies have been deployed for cooperative communications. Distributed space-time coding was originally proposed for MIMO systems [6]; nevertheless, synchronization among cooperative nodes is the unavoidable problem when the space-time coding strategy is brought into cooperative communications. Lately, as the network grows, traditional relay schemes have become increasingly bandwidth-inefficient. To break through the bandwidth bottleneck, network coding [11]—a technique originally developed for routing in lossless wireline networks—has been recently applied to wireless

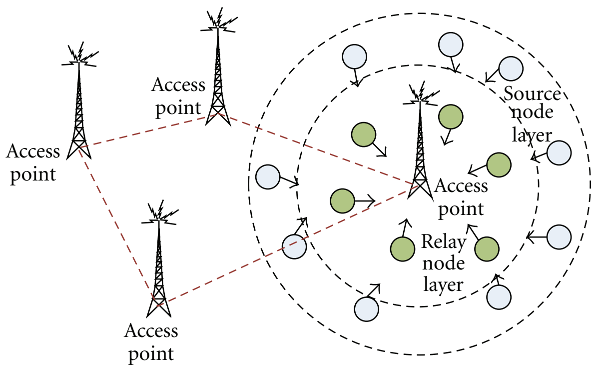

FIGURE 1: Hierarchical communication structure with multiple sources and dedicated relays.

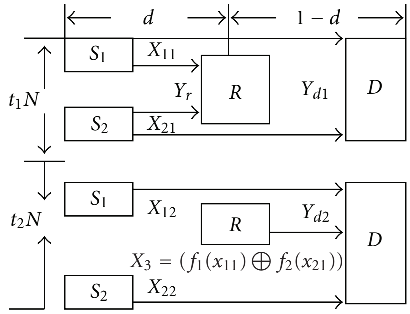

FIGURE 2: Cooperative protocol in MARC with one-block transmission. In the t_1 slot, S_1 and S_2 broadcast x_{11} and x_{21}; in the t_2 slot, R forwards the network-coded message x_3, and S_1 and S_2 transmit x_{12} and x_{22}.

relay networks. Traditional relaying [12–14] entails a loss in spectral efficiency that can be mitigated through network coding in cooperative communications, for its information theoretical scheme and cooperative nature. However, certain fundamental aspects of wireless communication, interference, fading, and mobility make the problem of applying network coding to cooperative communications particularly challenging.

The application of a cooperative network coding strategy is based on the fact that network coding has automatically been associated with cooperative communications as it employs intermediate nodes to combine packets [15–22]. Some approaches with practical advantages have been established to introduce network coding strategies into relay cases. In a two-way relay channel, the relay node combines received messages via network coding and broadcasts them to the opposite sited sources [15, 16]. Such a strategy has been demonstrated to reduce the number of time slots required to exchange a packet from 4 to 2, and thus a significant gain in throughput. A recently developed idea based on joint network coding with channel coding or source coding [17, 18, 21, 22] suggests that network coding is a generalization of source coding and channel coding [23]. Effros et al. [19] used network information theory to show that joint design of source, channel, and network coding in end-to-end transmission could yield much better performance, especially for the situation in which source, channel, and network separation between these codes does not hold in underlying networks.

In essence, the contribution of this paper is to employ network coding with additional parity-check bits generated from the two sources' information bits in relay nodes with linear acceptable complexity. The extra parity-check bits are designed as side information to fill up the mutual information gap between Source-Destination and Relay-Destination transmissions and hence approach the MARC "Cut-Set" bound, which is not addressed in most of the previous research works. Specifically, this paper constructs a multidimensional LDPC code to realize the network coding in a cooperative pair of nodes, as the graphical description of LDPC can flexibly bridge distributed processing and can be customized to emulate a random coding scheme of any rate. Although density evolution (DE) has high precision, the resulting increase in the complexity of DE poses a significant challenge to design a multidimensional LDPC decoder. Our work concentrates on practical implementation to present the behaviors of constituent decoders by Extrinsic Information Transfer Charts (EXITs) with a modified Gaussian approximation, which reduces the infinite dimensional problem of tracking densities to a one-dimensional problem of tracking means that is readily addressed with linear programming tools.

The remainder of the paper is organized as follows. Section 2 describes a MARC model as well as system settings. In Section 3, we analyze the achievable sum-rate with information theory as the motivation for coding design and propose network-coding cooperative transmit strategy with multidimensional LDPC codes. The work in Section 4 focuses on the optimization of multidimensional LDPC code profile using modified Gaussian approximation and EXIT as a linear-constraint optimization. Finally, simulations are conducted and discussed to demonstrate the effectiveness of the network-coded cooperative strategy.

2. System Model and Coding Strategy

This section briefly introduces the two-source MARC model used throughout the paper and LDPC code preliminaries as the basis of the paper.

2.1. System Model. To exhaustively describe the network coding strategy, we formulate our system to MARC, a model for network topologies in which multiple sources communicate with a single Destination in the presence of a Relay node. Basically, the system consists of two Sources (S_1, S_2), one Relay (R) and one Destination (D), as in Figure 2. This MARC model has a symmetric positioning of S_1, S_2 with respect to R and D. The relay moves along the line connecting D with the origin, which is normalized to 1. The distance between S and R is set to d. Path loss is proportional to $1/d^2$. The channels between each node are independent of each other. Perfect global channel knowledge is assumed at all nodes.

Since radio terminals cannot transmit and receive simultaneously in the same frequency band, most cooperative strategies are based on the half-duplex mode [24]. The nodes are allocated orthogonal channels by TDMA. S_1 and S_2 are assumed to send messages with no priority. One block transmission is separated into two consecutive time slots, normalized to $t_1 + t_2 = 1$. Furthermore, one block length of the source is N (for brevity and clarity, the symbols S_1 and S_2 are equal to and independent of each other) and is further divided into two subblocks with t_1N and t_2N-long codewords for two slots' transmissions.

We use X, Y to represent the signals sent and received. In particular, x_{ij}, $i, j \in \{1, 2\}$ denotes the signals sent by S_1, S_2. The subscript i identifies S_1 and S_2, and the subscript j represents the two consecutive channels. x_3 is the signal sent by R, and y_r is the signal received by R. The variables y_{d1} and y_{d2} are signals received by D in consecutive channels. Specifically, in time slot t_1, S_1 and S_2 broadcast their messages x_{11} and x_{21} to R and D. In time slot t_2, R forwards the network-coded message x_3, and S_1 and S_2 send the messages x_{12} and x_{22} (new or old) to D, as in Figure 2. The equivalent baseband transmission model is shown in (1):

$$\begin{aligned} y_r &= h_{s_1 r}x_{11} + h_{s_2 r}x_{21} + w_{r1}, \\ y_{d1} &= h_{s_1 d}x_{11} + h_{s_2 d}x_{21} + w_{d1}, \\ y_{d2} &= h_{s_1 d}x_{12} + h_{s_2 d}x_{22} + h_{rd}x_3 + w_{d2}. \end{aligned} \tag{1}$$

Rayleigh flat fading is adopted to model these links. Specifically, h_{ij} are channel coefficients capturing the effects of path-loss, shadowing, and fading, modeled by independent circularly symmetric complex Gaussian random variables with a mean of zero and a variance of σ_{ij}^2. Furthermore, w_i, $i = r$, d_1, and d_2 account for noise and other additive interferences at the receiver, modeled with an independent, zero-mean additive Gaussian white noise with variance σ^2.

2.2. Power Control. The transmit power of each source $P_i^t = E[(x_i(n)^2)]$, where $i = 1, 2, 3$ denote S_1, S_2, and R, respectively, is constrained by

$$\begin{aligned} P_1^{t_1} + P_2^{t_1} &\le P_{\text{tot}}^{t_1}, \\ P_1^{t_2} + P_2^{t_2} + P_3^{t_2} &\le P_{\text{tot}}^{t_2}. \end{aligned} \tag{2}$$

2.3. LDPC Codes. The cooperative coding scheme adopts LDPC code. A binary LDPC code is represented by a binary sparse parity-check matrix $\mathbf{H}_{k\times n}$ which connects to a bipartite graph with n variable nodes (corresponding to n columns) and k check nodes (corresponding to k rows). An attractive property of LDPC is that it can be designed graphically by a bipartite graph, which naturally matches the network topology for cooperation. The LDPC code is presented by its variable and check nodes degree distributions $(\lambda(x), \rho(x))$, where $\lambda_i(\rho_i)$ represents the fraction of edges connected to a variable (check) node with degree i. The rate of the code is given in terms of $(\lambda(x), \rho(x))$:

$$R = 1 - \frac{\int \rho(x)dx}{\int \lambda(x)dx}. \tag{3}$$

3. Parity-Check Network Code Design

There are two particular highlights of our cooperative strategy: one is the cooperative design of side information at the relay node to exactly fill up the gap of mutual information between SR and SD channels (based on the MARC model, relay is in the middle of S_1, S_2, and D, and SR thus subject to less path loss than SD channel); the other is the network coding procedure to combine extra check bits for one-slot transmission. Particularly, the insight of the first highlight is to approach the MARC DF "Cut-Set" bound, and the second is to ensure BER QoS as network coding is extended to wireless fading environment. This section will address these two challenges.

3.1. Achievable Rates. This subsection analyzes the parity-check network coding cooperative strategy, extended from *decode-and-forward* in MARC using information theory, as a fundamental instruction to develop the coding design as described below.

The key element in the proposed strategy is that the relay node forwards redundant bits as side information for both S_1 and S_2 to D, which is based on the essential idea of "channel coding with side information." This process is a "dual thought" of "source coding with side information" [25, 26]. Channel coding with side information is to append some extra check bits to codewords, which is a "binning" process assigning a set of codewords to different bins and enlarging the minimum distance between them. At the receiver, the side information provides an index of the message, and then the decoding process chooses the closest codeword in a box with a specific index. Application of such an idea in a traditional three-node relay network can be found in [8, 9]. This paper applies the binning approach to a MARC with network coding. Besides, the extra check bits are generated with the goal of approaching MARC DF capacity. The resulting network-coded strategy is capable of balancing the problem of spatial diversity and multiplexing.

Usually, the informational theoretical view deals with achievable rates. In the MARC scenario, we consider the sum-rate, which conveys more intuition. For *decode-and-forward* strategy in a general multiple source half-duplex relay channel, the bounds on all combinations of the rate tuples for reliable detection at R and D are as follows [1]:

$$\begin{aligned} &(R_{S_1} + R_{S_2})_{\text{DF}} \\ &\quad \le \min_{t_1+t_2=1} \begin{pmatrix} t_1 I(X_{11}, X_{21}; Y_r) + t_2 I(X_{12}, X_{22}; Y_{d_2} \mid X_3), \\ t_1 I(X_{11}, X_{21}; Y_{d_1}) + t_2 I(X_{12}, X_{22}, X_3; Y_{d_2}) \end{pmatrix}. \end{aligned} \tag{4}$$

The first terms in $\min(\cdot)$ of (4) represent the maximum rate at which R can decode the messages x_{11} and x_{21} and

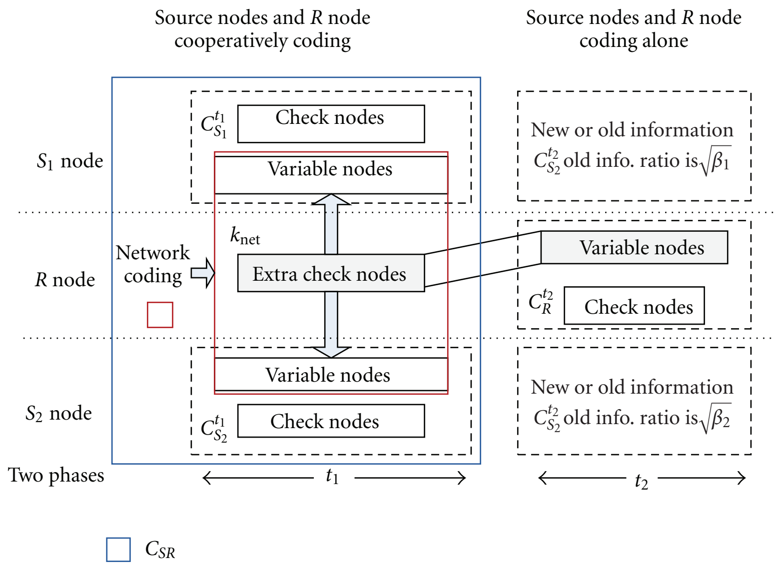

Figure 3: The cooperative strategy based on parity-check network coding.

the maximum rate at which D can decode x_{12} and x_{22} in the presence of x_3. The second terms in $\min(\cdot)$ of (4) represent the maximum rate at which D can decode the messages x_{11} and x_{21}, and the maximum rate at which D can decode all three messages x_{12}, x_{22}, andx_3.

The cooperative strategy in this study employs network coding in the sense of cooperation between S_1, S_2, and R to achieve MARC capacity in (4). The detailed protocol is as follows.

3.1.1. In Time Slot t_1: Source Nodes Operations. Each S_1 (S_2) encodes the message x_{11} (x_{21}) to codewords $C_{S_1}^{t_1}$ ($C_{S_2}^{t_1}$) at the rate of

$$R_{S_1R}^{t_1} + R_{S_2R}^{t_1} = I(X_{11}, X_{21}; Y_r). \quad (5)$$

Then, S_1 (S_2) broadcasts $C_{S_1}^{t_1}$ ($C_{S_2}^{t_1}$) to R and D. D receives the data and waits for decoding at the end of the block transmission.

To achieve maximum throughput, S_1 and S_2 broadcast messages at the sum-rate (5). R is able to decode x_{11}, x_{21} with an arbitrarily low error probability, since $R_{S_1R}^{t_1} + R_{S_2R}^{t_1}$ equals the capacity of the SR channels. According to the geometric configuration in Figure 2, intuitively, $I(X_{11}, X_{21}; Y_r) > I(X_{11}, X_{21}; Y_d)$; the physical channel of SD is more attenuated by the path loss than that of the SR channel. Consequently, although D also receives x_{11} and x_{21}, it is unable to uniquely decode them and requires extra bits $t_1N(I(X_{11}, X_{21}; Y_r) - I(X_{11}, X_{21}; Y_d))$ to make x_{11} and x_{21} decodable.

3.1.2. In Time Slot t_2: Relay Node Operation. R sends these extra bits, $t_1N(I(X_{11}, X_{21}; Y_r) - I(X_{11}, X_{21}; Y_d))$, to D at the rate

$$\begin{aligned} R_{RD} &= \frac{t_1N(I(X_{11}, X_{21}; Y_r) - I(X_{11}, X_{21}; Y_{d_1}))}{t_2N} \\ &= \frac{t_1}{t_2}(I(X_{11}, X_{21}; Y_r) - I(X_{11}, X_{21}; Y_{d_1})). \end{aligned} \quad (6)$$

Specifically, after decoding the codewords from S_i, R estimates $C_{S_1}^{t_1}$ and $C_{S_2}^{t_1}$, and cooperatively uses the codewords $C_{S_1}^{t_1}$ and $C_{S_2}^{t_1}$ to generate extra check bits for both S_1 and S_2, and then combines them with network coding to produce $k_{net} = t_1N(I(X_{11}, X_{21}; Y_r) - I(X_{11}, X_{21}; Y_{d_1}))$ extra check bits. The process is "network coding." For transmission, k_{net} is encapsulated by R's LDPC codeword $C_R^{t_2}$ and sent to D. Hence, the extra check bits with S_1 and S_2 codes $C_{S_1}^{t_1}$ and $C_{S_2}^{t_1}$ construct the cooperative multidimensional LDPC code C_{SR}, as illustrated in Figure 3. The elements in the blue rectangle construct the cooperative code C_{SR} with respect to the information in time slot t_1. The procedure in the red rectangle is the network coding which produces and combines extra bits for both S_1 and S_2. In particular, k_{net} check bits encapsulated by codeword $C_R^{t_2}$ sent to D capture the RD channel's fading characteristics and provide an effective extinct message at D to realize a spatial diversity.

From the perspective of information theory, C_{SR} is cooperatively encoded by S_1, S_2, and R on the grounds of coding with side information. "Binning" is performed by extra check network-coded bits (or syndromes) in R's message generated from $C_{S_i}^{t_1}$, $i \in \{1,2\}$ to perform decoding of $x_{11}, x_{21} \in \{1, 2, \ldots, 2^{t_1NI(X_{11}, X_{21}; Y_r)}\}$ by restricting them into $2^{t_1NI(X_{11}, X_{21}; Y_{d_1})}$ bins of $2^{t_1N(I(X_{11}, X_{21}; Y_r) - I(X_{11}, X_{21}; Y_{d_1}))}$ in size each. From Figure 4, the "binning" process of R partitions the space of codewords of S_1 and S_2, enlarging their minimum distances to make the source's message decodable.

3.1.3. Source Nodes Operations. In time slot t_2, each S_1 (S_2) sends a message to D independently because R is in the half-duplex mode. According to the channel status, S_1 and S_2 can choose to send new or old information using the independent codebook $C_{S_1}^{t_2}$ ($C_{S_2}^{t_2}$). The new information sent

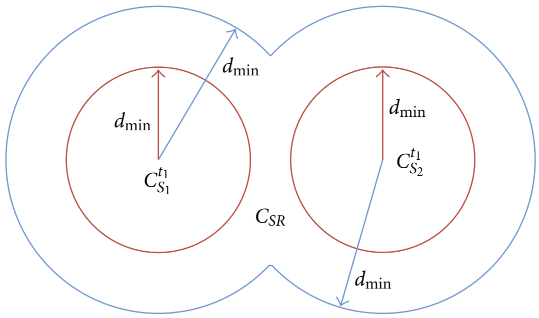

FIGURE 4: The minimum distances of C_{SR} and $C_{S_i}^{t_1}$, $i \in \{1,2\}$.

in the t_2 time slot at the sum-rate inherited from the DF rate region in (4) is

$$\left(R_{S_1D}^{t_2} + R_{S_2D}^{t_2}\right)_{\mathrm{DF}} \le \min\left(\begin{array}{c} I(X_{12}, X_{22}; Y_{d_2} \mid X_3), \\ \left(\begin{array}{c} I(X_{12}, X_{22}, X_3; Y_{d_2}) \\ -\dfrac{t_1}{t_2}\left(I(X_{11}, X_{21}; Y_r) - I(X_{11}, X_{21}; Y_{d_1})\right) \end{array}\right) \end{array}\right). \quad (7)$$

Source transmissions in the t_2 slot are isolated from the operation of R, as in Figure 3, which illustrates the operation in time slot t_2 with independent information transmissions by S_1, S_2, and R. Thus, we deal with codebook $C_{S_1}^{t_2}$ ($C_{S_2}^{t_2}$) as a single LDPC code and choose a suitable LDPC codebook to satisfy the rate constraint in (7).

At the end of one block transmission, D successively decodes $C_R^{t_2}$, $C_{S_1}^{t_2}$, and $C_{S_2}^{t_2}$. Then, the extra check bits k_{net} are obtained for joint decoding of C_{SR} with $C_{S_1}^{t_1}$ and $C_{S_2}^{t_1}$.The network coding cooperative strategy is summarized as follows in Table 1.

In the cooperative protocol mentioned above, MARC DF capacity in (4) is approximated via the rate allocation scheme in (5) through (7). Especially, if $I(X_{11}, X_{21}; Y_r) > I(X_{11}, X_{21}; Y_d)$, the rate at $I(X_{11}, X_{21}; Y_r)$ to transmit information of S_1 and S_2 in time slot t_1 to D will be achieved, resulting in a rate gain by cooperation between S_1, S_2, and R.

However, strictly speaking, the network coding performed here is not exactly the same as the network layer coding, which mainly focuses on routing problems and packet-level combination. Here, we borrow the kernel idea of the network layer coding to combine the extra check bits in R, which improves the bandwidth efficiency by R's extra check bits transmitted in one slot for both S_1 and S_2.

3.1.4. Parameters in the Cooperative Protocol. The achievable sum-rate is as a function of three parameters: d, t_1, and β_i. The definition of d and t_1 is in Section 2.1. β_i is the fraction of S_i allocate to the old messages in t_2. And $\beta_1 = \beta_2 = \beta$ is set for the symmetric geometry. The achievable sum-rate in (4) can be evaluated by these three parameters with the AWGN channel capacity. The outer bound of the sum-rate is the maximum of (8) subject to the value of $t_i\beta_i$, $i \in \{1,2\}$.

$$\begin{aligned} &(R_{S_1} + R_{S_2})_{\mathrm{DF}} \\ &\le \max_{t_i,\beta_i}\left\{\min\left(\begin{array}{c} \left(\begin{array}{c} t_1 C\left(\sum\limits_{i\in\{1,2\}} \gamma_{S_i}^{t_1} |h_{S_i r}|^2\right) \\ +t_2 C\left(\sum\limits_{i\in\{1,2\}} (1-\beta_i)\gamma_{S_i}^{t_2} |h_{S_i d}|^2\right) \end{array}\right), \\ \left(\begin{array}{c} t_1 C\left(\sum\limits_{i\in\{1,2\}} \gamma_{S_i}^{t_1} |h_{S_i d}|^2\right) \\ +t_2 C\left(\sum\limits_{i\in\{1,2\}} \gamma_{S_i}^{t_2}|h_{S_i d}|^2 + \gamma_R^{t_2}|h_{rd}|^2 + \sum\limits_{i\in\{1,2\}} 2\sqrt{\beta_i \gamma_{S_i}^{t_2}|h_{S_i d}|^2 \gamma_R^{t_2}|h_{rd}|^2}\right) \end{array}\right) \end{array}\right)\right\}. \end{aligned} \quad (8)$$

The received signal-to-noise ratio for R and D is listed with the channel gains as

$$\begin{array}{ll} P_{S_i r}^{t_1} = \gamma_{S_i}^{t_1} |h_{S_i r}|^2, & P_{S_i d}^{t_1} = \gamma_{S_i}^{t_1} |h_{S_i d}|^2, \\ P_{S_i d}^{t_2} = \gamma_{S_i}^{t_2} |h_{S_i d}|^2, & P_{rd}^{t_2} = \gamma_R^{t_2} |h_{rd}|^2, \end{array} \quad i \in \{1,2\}. \quad (9)$$

$\gamma = E_S/\sigma^2 = P/(W\sigma^2)$ is the input signal-to-noise ratio (SNR), where power P is constrained within 10 dB in both time slots using (2), and σ^2 is the variance of noise at the receivers of R and D, which are assumed to be equal.

The rates of (8) are plotted in Figure 5. Note that, when d is around 0.5, the sum-rate is at its maximum. The function of best β against d is more like a step function. When R is physically closer to the source $d < 0.3$, $\beta = 1$ is optimal, which means that the old information takes up all source transmissions in time slot t_2. This could be attributed to a path loss of the RD channel, and so S_1 and S_2 send the same information again to fill up the gap. The other extreme is when R is physically closer to D, $d > 0.7$, $\beta = 0$ which means that sources send new information in time slot t_2. However, R must successfully decode the source's information.

To obtain the time partition factor t_1, the sum-rate in (7) can be used to calculate t by manipulating the sum-rate at the corner point of the capacity region, which means that the two terms of min$(\cdot)$ in (7) are equal. In Figure 5, we evaluate t by setting the two terms mentioned above to be equal, with different d. When $d = 0.5$ and $t_1 = 0.7$, the MARC DF sum-rate achieves its maximum value, which means that R's transmission takes up $t_2 = 0.3$ slot, resulting in a free degree of each source of $0.7/2 + 0.3 = 0.65$.

3.2. Cooperative Design Framework. This subsection depicts the network-coded cooperative framework to realize above achievable rates. Specifically, the layered structure is constructed with multidimensional LDPC constituent codes corresponding to S_1 and S_2, as in Figure 6. This coding strategy is based on a half-duplex TDD mode, so that the

Table 1: The network-coded cooperative strategy.

	S_1 and S_2	R	D
t_1	Broadcast $C_{S_1}^{t_1}$ and $C_{S_2}^{t_1}$	Receives $C_{S_1}^{t_1}$ and $C_{S_2}^{t_1}$ Performs network coding to generate k_{net} extra check bits which is encoded by $C_R^{t_2}$ and sends $C_R^{t_2}$ to D	Receives $C_{S_1}^{t_1}$ and $C_{S_2}^{t_1}$ and stores them for deocoding.
t_2	Send $C_{S_1}^{t_2}$ and $C_{S_2}^{t_2}$ to D.		(1) Receives $C_{S_1}^{t_2}$ and $C_{S_2}^{t_2}$ (2) Receives $C_R^{t_2}$ (3) Successively decodes $C_{S_1}^{t_2}, C_{S_2}^{t_2}, C_R^{t_2}$ and obtains k_{net} (4) Joint decodes $C_{S_1}^{t_1}$ and $C_{S_2}^{t_1}$ with k_{net}

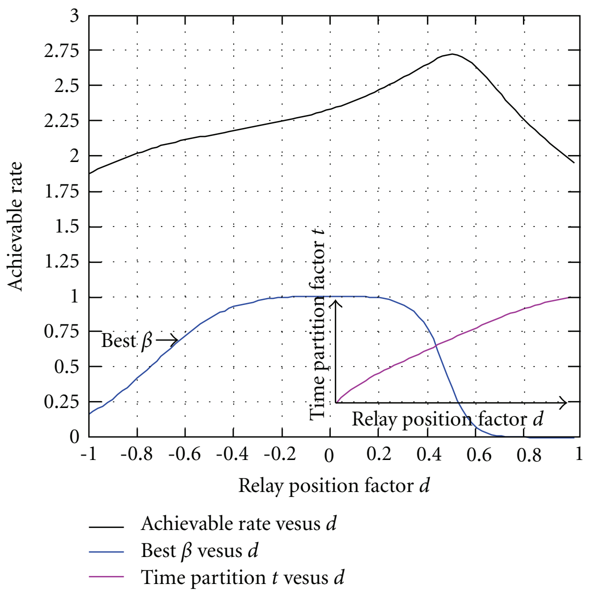

Figure 5: The achievable sum-rate with $P_1^{t_1} + P_2^{t_1} \leq P_{\text{tol}}^{t_1} = 10\,\text{db}$, $P_1^{t_2} + P_2^{t_2} + P_3^{t_2} \leq P_{\text{tol}}^{t_2} = 10\,\text{db}$.

operation of R only cooperates with the source transmissions in time slot t_1. In time slot t_2, S_1, S_2, and R send their information independently.

The cooperative codeword C_{SR}'s parity-check matrix $\mathbf{H}_{SR}$ is constructed with three LDPC constituent codes as in Figure 6, including sub-LDPC parity-check matrices $\mathbf{H}_{S_1}$ and $\mathbf{H}_{S_2}$, and the network code parity-check matrix $\mathbf{H}_{\text{net}}$. $\mathbf{H}_{S_1}$ ($\mathbf{H}_{S_2}$) is employed by S_1 (S_2) to encode the message x_{11}, (x_{21}) locally; thus, $\mathbf{H}_{S_1}$ ($\mathbf{H}_{S_2}$) is a complete parity-check matrix. $\mathbf{H}_{S_1}$ ($\mathbf{H}_{S_2}$) has n_1 (n_2) variable nodes and k_1 (k_2) check nodes. The sources' codeword $C_{S_1}^{t_1}$ ($C_{S_2}^{t_1}$) is enforced to satisfy k_1 (k_2) check bits.

In addition, parity-checks k_1 and k_2 do not interact with each other or do not check each others' variable nodes since the independent sources S_1 and S_2 cannot produce checks for unknown information bits.

The extra check nodes k_{net} have the same variable nodes as the check nodes of S_1 and S_2; otherwise, they cannot provide any checks for the codewords of S_1 and S_2. Therefore, in $\mathbf{H}_{\text{net}}$, the variable nodes n_1 and n_2 are sequentially arranged as information bits and are enforced to satisfy k_{net} check bits. Hence, $\mathbf{H}_{\text{net}}$ has k_{net} rows and $(n_1 + n_2 + k_{\text{net}})$ columns, as $\mathbf{H}_{\text{net}}$: $k_{\text{net}} \times (n_1 + n_2 + k_{\text{net}})$. Above all, the network coding procedure uses $\mathbf{H}_{\text{net}}$ to merge the extra check bits.

Random linear codes are capacity-approaching for the Gaussian channel under maximum likelihood decoding. Therefore, the extra checks are randomly connected to the set of variable nodes $n_1 + n_2$ in $\mathbf{H}_{\text{net}}$. However, if $\mathbf{H}_{\text{net}}$ is constructed in a completely random way, encoder and decoder implementations become very difficult as the code size grows due to the pseudorandom interconnection and the large memory required. Structured LDPC codes would be a good option to facilitate implementation without compromising performance. Therefore, $\mathbf{H}_{\text{net}}$ is constructed in the partial dual-diagonal form so that most parity check bits can be obtained via back-substitution. Partial dual-diagonal form is merely in the k_{net} portion, as illustrated in Figure 6, and the remainders are still randomly constructed.

Linear-time encoding can be achieved by using the near-triangular parity portion. The extra check bits $b_1, b_2, \ldots, b_{k_{\text{net}}}$ are generated by a direct encoding procedure, as follows:

$$
\begin{aligned}
b_0 &= \sum_{j=1}^{t_1 N + t_1 N} \sum_{i=1}^{k_{\text{net}}} H_{\text{net}}(i, j)\left[C_{S_1}^{t_1}, C_{S_2}^{t_1}\right]^T, \\
b_1 &= \sum_{j=1}^{t_1 N + t_1 N} H_{\text{net}}(i, j)\left[C_{S_1}^{t_1}, C_{S_2}^{t_1}\right]^T + b_0, \quad i = 1, \\
b_{i+1} &= b_i + \sum_{j=1}^{t_1 N + t_1 N} H_{\text{net}}(i, j)\left[C_{S_1}^{t_1}, C_{S_2}^{t_1}\right]^T + b_0, \\
&\qquad i = 2, \ldots, k_{\text{net}}.
\end{aligned}
\tag{10}
$$

The addition of the above equations is in a binary field; b_0 is an additional variable used to calculate extra check bits $b_1, b_2, \ldots, b_{k_{\text{net}}}$.

As mentioned above, the cooperative LDPC code C_{SR} is satisfied by the parity-check constraints as

$$
\begin{gathered}
H_{S_1}\left[C_{S_1}^{t_1}\right] = 0; \qquad H_{S_2}\left[C_{S_2}^{t_1}\right] = 0; \\
H_{SR}\left[C_{S_1}^{t_1}, C_{S_2}^{t_1}, \{b_1, b_2, \ldots, b_{k_{\text{net}}}\}\right] = 0.
\end{gathered}
\tag{11}
$$

Moreover, once k_{net} extra check bits are obtained via optimization cooperatively conducted with $\mathbf{H}_{S_1}$ and $\mathbf{H}_{S_2}$, the quasidiagonal part of $\mathbf{H}_{\text{net}}$ is determined. Hence the parity-check matrix $\mathbf{H}_{SR}$ can be simplified to $\mathbf{H}'_{SR}$ by removing the columns of the quasidiagonal part, and the optimization is then performed on $\mathbf{H}'_{SR}$ instead.

In $\mathbf{H}'_{SR}$, variable nodes have two types of checks: their own checks and extra checks offered by network coding.

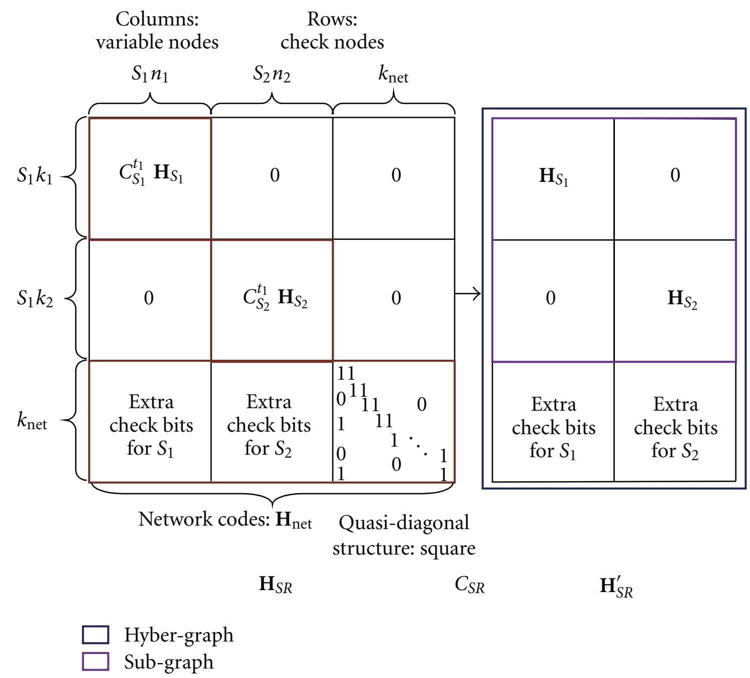

Figure 6: The cooperative design framework of parity-check network coding.

Accordingly, each variable node in $\mathbf{H}'_{SR}$ has two types of variable node degrees, expressed by $\lambda_{i,j}^{SR}$: sub-LDPC degree (in $\mathbf{H}_{S_1}$ or $\mathbf{H}_{S_2}$) i, $i \geq 2$, and extra degree j, $j \geq 0$ (in $\mathbf{H}_{net}$). Assuming that $0 < \eta_1(\eta_2) < 1$ is the ratio of the edges in $\mathbf{H}_{S_1}$ ($\mathbf{H}_{S_2}$) to the edges in $\mathbf{H}'_{SR}$, the variable node degree distributions $\gamma^{S_1}(x)$ ($\gamma^{S_2}(x)$) of $\mathbf{H}_{S_1}$ ($\mathbf{H}_{S_2}$) in terms of $\lambda_{i,j}^{SR}$ are

$$\gamma_i^{S_1} = \frac{1}{\eta_1}\sum_{j\geq 0}\frac{i}{i+j}\lambda_{i,j}^{SR}, \qquad \gamma_i^{S_2} = \frac{1}{\eta_2}\sum_{j\geq 0}\frac{i}{i+j}\lambda_{i,j}^{SR}. \tag{12}$$

The relationship of (12) is used for cooperative code profile optimization in next section.

Then, we will give the kernel constraint of the cooperative design, which determines how the extra check bits are connected to the variable node set in the cooperative code C_{SR}. Since the extra checks are appended to the sub-LDPC codes $C_{S_1}^{t_1}$ and $C_{S_2}^{t_1}$, which have the same set of variable nodes as C_{SR}, the degree of C_{SR} variable nodes turns out to be greater than that of the same set of variable nodes in sub-LDPC codes $C_{S_1}^{t_1}$ and $C_{S_2}^{t_1}$. However, due to the random construction, the extra checks connected to one specific variable node cannot be determined; in other words, it is impossible to list exactly which variable node receives the extra checks. Under this circumstance, we derive the relationship between $C_{S_1}^{t_1}$, $C_{S_2}^{t_1}$, and C_{SR} in terms of variable nodes' number with respect to a specific degree i, denoted by $N_i = (\lambda_i/i)\cdot E$, where E is the total number of edges of the parity-check matrix concerned.

Theorem 1. *If the cooperative code C_{SR} has a maximum degree $d_{v,SR}$ and a total number of edges E_{SR} and, similarly, two sub-LDPC codes $C_{S_1}^{t_1}$ and $C_{S_2}^{t_1}$ have maximum degrees d_{v,S_1} and d_{v,S_2} and total edges E_{S_1} and E_{S_2}, respectively, then one has the following relationships:*

$$\sum_{i=j}^{d_{v,SR}}\frac{\lambda_{i,j}^{SR}}{i}E_{SR} \geq \sum_{i=j}^{\max(d_{v,S_1},d_{v,S_2})}\left(\frac{\gamma_i^{S_1}}{i}E_{S_1}+\frac{\gamma_i^{S_2}}{i}E_{S_2}\right) \quad \forall j = 2,3,\ldots,d_{v,SR}. \tag{13}$$

The proof of Theorem 1 is in the appendix. Theorem 1 ensures that the network-coded messages from the relay node as the extra check bits independently sent through the fading channel offer spatial diversity gain to the cooperative strategy. And the number of extra check bits is determined by

$$(n_1+n_2)\left(I(X_{11},X_{21};Y_r) - I(X_{11},X_{21};Y_{d_1})\right). \tag{14}$$

4. Cooperative Code Profile Optimization

Next, the challenge to the construction of $\mathbf{H}'_{SR}$ lies in finding the optimal code profile of C_{SR}, including optimal profiles of sub-LDPC constituent codes $C_{S_1}^{t_1}$, $C_{S_2}^{t_1}$ together with extra check bits.

In engineering, optimization has always been a difficult problem due to its computational complexity, particularly for cost-constraint hardware. Therefore, to restrict our optimization algorithms to a linear programming is the mainly interest in this section. We will use Gaussian approximation and Extrinsic Information Transfer (EXIT) charts as the linear programming tool to obtain a C_{SR} code profile in a cooperative framework illustrated in Figure 6.

Generally, optimization of LDPC code profile can be done in two different ways. One is to fix noise variance and maximize information transmit rate to search for the optimal degree distributions $(\lambda(x), \rho(x))$. The other is to fix the rate to find the $(\lambda(x), \rho(x))$ that yields the largest noise threshold. The cooperative strategy discussed in this paper prefers bandwidth efficiency to noise threshold. Information transmit rate seems straightforward, which is defined as the ratio of information bits sent by sources to all bits transmitted for the concerned message (source messages in time slot t_1), and thus,

$$R_{SR} = \frac{n_1 - k_1 + n_2 - k_2}{n_1 + n_2 + k_{\text{net}}}. \tag{15}$$

Equation (15) can be expressed by the degree distribution as

$$R_{SR} = 1 - \frac{\sum_{i\geq 2} \rho_i^{SR}/i}{\sum_{i\geq 2, j\geq 0} \lambda_{i,j}^{SR}/(i+j)}. \tag{16}$$

The optimization algorithm maximizes rate R_{SR} to obtain the degree distribution of $\mathbf{H}'_{SR}$.

It is difficult to obtain $(\lambda(x), \rho(x))$ in one operational procedure, and so we fix $\rho(x)$ to get $\lambda(x)$ and then get $\rho(x)$ with fixed $\lambda(x)$, given the maximum number of iterations. With a constant $\rho(x)$, the maximizing rate is equivalent to maximizing $\sum_{i\geq 2, j\geq 0} \lambda_{i,j}^{SR}/(i+j)$.

EXIT [27] provides a computationally simple tool for predicting the asymptotic convergence behavior of iterative coding schemes by tracking trajectories of extrinsic information exchange between variable nodes and check nodes in the bipartite graph. Furthermore, operations of variable and check nodes are referred to the variable-node decoder (VND) and check-node decoder (CND), respectively. We also use mutual information as the surrogate to analyze and optimize LDPC codes by matching the EXIT functions with the constituent decoders (VND, CND) based on the area property of the functions. Figure 7 illustrates iterative joint decoding of VND and CND in $\mathbf{H}'_{SR}$. Specifically, $C_{S_1}^{t_1}$ and $C_{S_2}^{t_1}$ are received by D at t_1 time slot, while $C_R^{t_2}$ is received by D at t_2 time slot. Channel S_1D captures its own fading factor via $C_{S_1}^{t_1}$; channel S_2D captures its own fading factor via $C_{S_2}^{t_1}$; channel RD captures its own fading factor via $C_R^{t_2}$. These three codewords are used to cooperative decode x_{11} and x_{21}. Each sub-LDPC code is related to a coupling of a VND-CND decoder. The network code plays a role as the interleaving function of the two CNDs with extra extrinsic information.

EXIT charts compute two curves, the VND curve and the CND curve, corresponding to the steps of each decoder's density evolution. With the VND curve, I_A is interpreted as the mutual information between the VND "input" LLR message and the transmitted symbol of the check node at iteration l. I_E is interpreted as the mutual information between the VND "output" LLR message and the transmitted symbol of the variable node at iteration l. With the CND function, the interpretations of I_E and I_A are opposite.

Gaussian approximation is an effective way to track the means of the log likelihood ratio (LLR) message, which is assumed to be symmetrically Gaussian distributed [28]. Even with an irregular LDPC code [27], the Gaussian approximation can still be precise after a few modifications; that is, the distribution of the variable node LLR message is a mixture of Gaussian approximations, and the corresponding VND EXIT function is

$$\begin{aligned} I_{E_V} &= f(I_{ch}, I_{A_V}) = \sum_{j=2}^{d_v} \lambda_j I_{E_{Vj}} \\ &= \sum_{j=2}^{d_v} \lambda_j J\left(J^{-1}(I_{ch}) + (j-1)J^{-1}(I_{A_V})\right), \end{aligned} \tag{17}$$

where $J(x)$ is defined by

$$J(x) = I(X, L) = \int \frac{1}{\sqrt{4\pi x}} e^{-(l-x)^2/4x} \left(1 - \log_2\left(1 + e^l\right)\right) dl. \tag{18}$$

The corresponding CND EXIT function is

$$\begin{aligned} I_{E_c} &= f(I_{A_c}) = \sum_{j=2}^{d_c} \rho_j I_{E_{cj}} \\ &= \sum_{j=2}^{d_c} \rho_j \frac{1}{\ln 2} \sum_{i=1}^{\infty} \frac{1}{(2i-1)(2i)} \left[\varphi_i\left(J^{-1}(I_{A_c})\right)\right]^{j-1}, \end{aligned} \tag{19}$$

where $\varphi_i(x)$ is defined by

$$\varphi_i(x) = \int_{-1}^{1} \frac{2t^{2i}}{(1-t^2)\sqrt{4\pi x}} e^{-(\ln(1+t/1-t)-x)^2/4x} dt. \tag{20}$$

The decoding process is expected to converge progressively after each decoding iteration. Therefore, we require $I_{E_v}(I_{E_c}(I_A)) > I_A$ for all $I_A \in [0,1]$ to ensure successful decoding. This is equivalent to $I_{E_v}(I_A) > I_{E_c}^{-1}(I_A)$. The decoding process is thus predicted to converge if and only if the VND curve is strictly greater than the reversed-axis CND curve.

Next we will formulate the constraints to fulfill the optimization and obtain code profiles of C_{SR}, $C_{S_1}^{t_1}$, and $C_{S_2}^{t_1}$: $(\lambda_{i,j}^{SR}, \rho^{SR})$, $(\gamma^{S_1}, \rho^{S_1})$, and $(\gamma^{S_2}, \rho^{S_2})$. In this paper, for simplicity but still revealing the insights of the cooperative design, we let node S_1 and S_2 completely symmetric, that is, $C_{S_1}^{t_1}$ and $C_{S_2}^{t_1}$ are equal, and thus in simulations we can treat them as one LDPC code $C_{S_1}^{t_1}$ (or $C_{S_2}^{t_1}$).

First, (13) in Section 3 is the kernel constraint. Specifically, if S_1 and S_2 are completely symmetric, which means that $C_{S_1}^{t_1}$ and $C_{S_2}^{t_1}$ have an equal number of extra checks and an equal number of bipartite graph edges, that is, $E_{SR} = 2E_{S_1} = 2E_{S_2}$, we have

$$\begin{aligned} &\sum_{i=j}^{d_{v,SR}} \frac{\left(\lambda_{i,j}^{SR}\right)}{i} \\ &\quad \geq \sum_{i=j}^{\max(d_{v,S_1}, d_{v,S_2})} \left(\frac{\gamma_i^{S_1}}{2i} + \frac{\gamma_i^{S_2}}{2i}\right) \quad \forall j = 2, 3, \ldots, d_{v,SR}. \end{aligned} \tag{21}$$

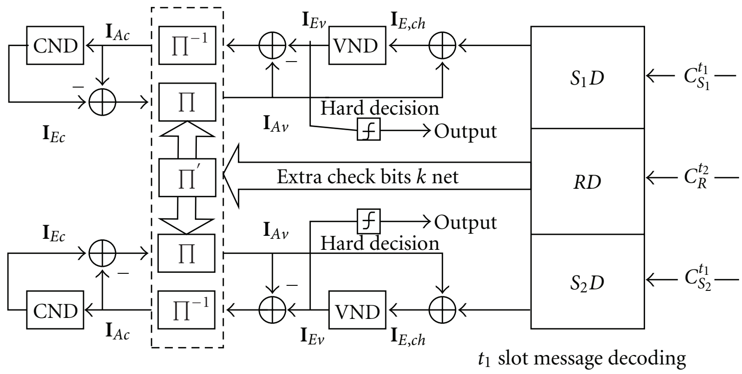

Figure 7: Decoder structure for joint decoding of C_{SR}.

Equation (21) poses a constraint to ensure the cooperative design of C_{SR} together with $C_{S_1}^{t_1}$ and $C_{S_2}^{t_1}$.

Moreover, the rate constraints are imposed to further restrict cooperative design. Cooperative C_{SR} has more check bits than both sources; so the cooperative code rate should be lower than any rate of S_1 and S_2:

$$R_{SR} < R_{(C_{S_1}^{t_1})}, \quad R_{SR} < R_{(C_{S_2}^{t_1})},$$
$$\left(R_{(C_{S_j}^{t_1})} = 1 - \left(\frac{\sum_i \rho_i / i}{\sum_i \gamma_i / i} \right)^{S_j}, \ j = 1, 2 \right). \tag{22}$$

As mentioned above, using EXIT, the VND curve must be strictly greater than the reversed-axis CND curve to ensure the convergence of a propagation decoding algorithm, which requires that all the constituent codes satisfy the condition $I_{E_v}(I_A) > I_{E_c}^{-1}(I_A)$, with additional irregular LDPC modification for all I belonging to a discrete, fine grid over (0, 1):

$$\begin{aligned} &\sum \gamma_i^{S_1} I_{E_V,i}^{S_1}(I_{A_V}, I_{ch}) > I^{-1}{}_{E_C}^{S_1}(I_{A_C}) + \delta, \\ &\sum \gamma_i^{S_2} I_{E_V,i}^{S_2}(I_{A_V}, I_{ch}) > I^{-1}{}_{E_C}^{S_2}(I_{A_C}) + \delta, \qquad \delta > 0, \\ &\sum_{i,j} \lambda_{i,j}^{SR} I_{E_V,i,j}(I_{A_V}, I_{ch}) > I^{-1}{}_{E_C}^{SR}(I_{A_C}) + \delta. \end{aligned} \tag{23}$$

Clearly, the degree distribution $\lambda(x)$ of a complete parity-check matrix sums to "1" wherever it occurs in $\mathbf{H}_{S_1}$ and $\mathbf{H}_{S_2}$ or in $\mathbf{H}'_{SR}$:

$$\gamma^{S_1}(1) = \gamma^{S_1}(1) = \lambda^{SR}(1) = 1. \tag{24}$$

The above four constraints (21)–(24) formulate the cooperative design and optimization and maintain the linear features of the variable node degree distribution $\lambda(x)$. Linear optimization with respect to $\lambda(x)$ yields a good C_{SR} profile $\lambda(x)$ with a fixed and concentrated check node degree $\rho(x)$. Meanwhile, fixing the variable node degree distribution $\lambda(x)$, similar optimization principles hold for the check node degree distribution $\rho(x)$.

5. Simulations and Results

This section validates the performance of parity-check network coding in MARC via numerical simulations. These simulations focus on two goals: (1) demonstrating that the cooperative framework produces a good cooperative code C_{SR} profile as well as a single code $C_{S_1}^{t_1}$ or $C_{S_2}^{t_1}$ profile and (2) investigating the BER performance of the cooperative code C_{SR} under different channel settings compared with $C_{S_1}^{t_1}$ or $C_{S_2}^{t_1}$.

5.1. EXIT Chats of Code Profile. EXIT charts of C_{SR}, $C_{S_1}^{t_1}$ (or $C_{S_2}^{t_1}$) are shown in Figure 8. With the rate $R_{S_1R}^{t_1} = 0.5$ ($R_{S_2R}^{t_1} = 0.5$) and the SNR = 1.2 dB, the EXIT curve of VND and CND is obtained. The curve of CND is strictly lower than the reversed-axis VND curve. Figure 8(b) draws the EXIT chart of the cooperative code C_{SR} subject to the EXIT chart of $C_{S_1}^{t_1}$ (or $C_{S_2}^{t_1}$) in Figure 8(a) with the linear optimization algorithm mentioned in Section 4. The curves of VND and CND approach asymptotically as the code rate increases. However, a comparison of the two subfigures shows that the gap between the VND and CND curves of C_{SR} is greater than that of $C_{S_1}^{t_1}$ (or $C_{S_2}^{t_1}$) because more check bits work on the same set of variable nodes for code C_{SR}. Table 2 lists the optimal degree distributions at the $C_{S_1}^{t_1}$ (or $C_{S_2}^{t_1}$) code rates of 0.3, 0.4, 0.5, and 0.6. In each column of the rate, $C_{S_1}^{t_1}$ (or $C_{S_2}^{t_1}$) code profile is in the left subcolumn, while the cooperative C_{SR} code profile is in the right subcolumn. It is obvious that the distributions satisfy the constraints of (21)–(24); this is especially true for the cooperative design constraints.

Moreover, Figure 9 shows the maximum of C_{SR} transmit rates and related $C_{S_1}^{t_1}$ (or $C_{S_2}^{t_1}$) transmit rates obtained by the linear optimization algorithm in Section 4. Here, we assume that the S_1 and S_2 have the same transmit rate (this is not necessary). We also plot the MARC *decode-and-forward* "Cut-Set" capacity in the same figure to compare the proposed parity-check network coding strategy. These results show that the cooperative strategy achievable rate is approximately 0.5 dB below the MARC capacity. And for better illustration the cooperative strategy, the direct link transmission capacity, that is, $I(X_{11}, X_{21}; Y_{d_1})$ without relay is also plotted.

Table 2: Code profile from the optimization algorithm.

Rate	0.3				0.4				0.5				0.6			
	$C_{S_1}^{t_1}$ (or $C_{S_2}^{t_1}$)		C_{SR}		$C_{S_1}^{t_1}$ (or $C_{S_2}^{t_1}$)		C_{SR}		$C_{S_1}^{t_1}$ (or $C_{S_2}^{t_1}$)		C_{SR}		$C_{S_1}^{t_1}$ (or $C_{S_2}^{t_1}$)		C_{SR}	
$\lambda(x)$	2	0.2264	2	0.1671	2	0.2479	2	0.1716	2	0.243	2	0.1956	2	0.3944	2	0.3463
	3	0.0173	3	0.0288	4	0.1395	4	0.1996	3	0.2994	3	0.1127	3	0.0462	3	0.0749
	4	5.03e-6	5	0.2689	5	0.2893	5	0.2887	7	0.2862	4	0.171	4	0.2411	4	0.2246
	5	0.2683	6	0.0338	18	0.0604	18	0.0539	8	5.98e-6	7	0.2304	5	0.3183	5	0.2086
	6	0.1074	8	0.0451	19	0.2629	19	0.1492	9	0.1714	8	4.63e-6			8	0.101
	27	0.1818	29	0.2256			27	0.0835	10	3.13e-6	9	0.0467			9	0.0446
	29	0.1273	30	0.1693			38	0.0535			23	3.12e-6				
	31	0.0259	31	0.0221							24	0.2434				
	58	0.0455	59	0.0394												
$\rho(x)$	3	0.0340	3	0.0592	5	0.2011	6	0.6623	6	0.2923	6	0.5084	7	0.6984	7	0.9667
	4	0.0634	4	0.0497	7	0.6084	7	0.0724	7	0.6073	7	0.3165	8	0.3016	20	0.0333
	6	0.2133	7	0.2295	13	0.1463	20	0.2653	20	0.1003	20	0.1751				
	8	0.4504	8	0.0310	16	0.0442										
	9	0.2091	10	0.5258												
	20	0.0298	20	0.1049												

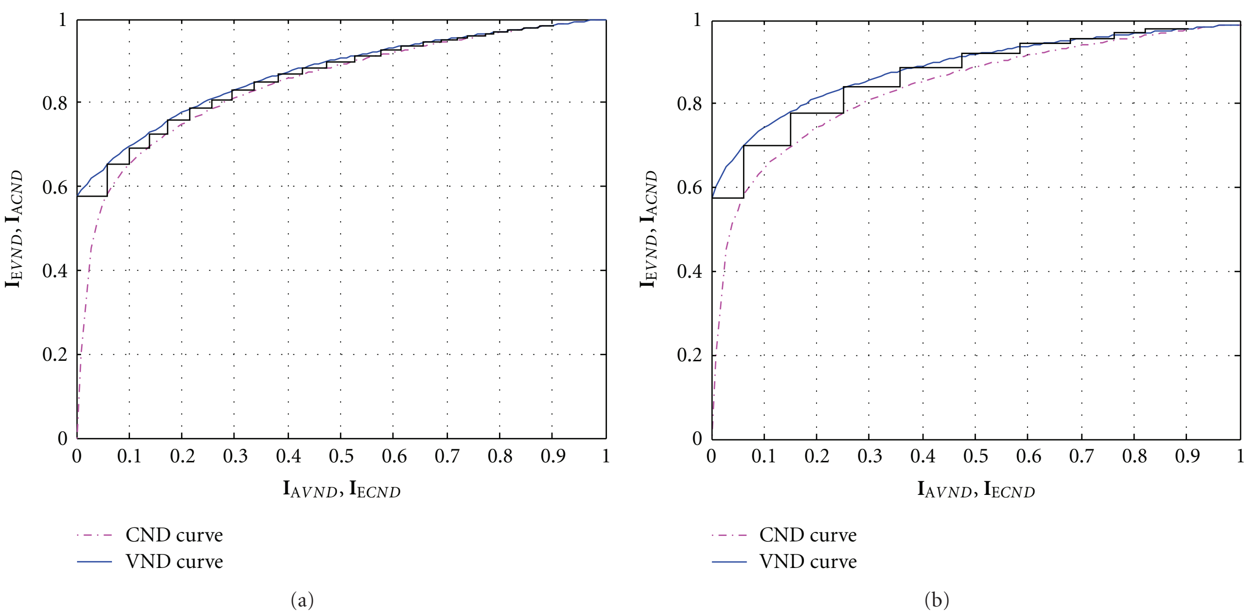

Figure 8: VND-CND decoding trajectory: (a) $C_{S_1}^{t_1}$ or $C_{S_2}^{t_1}$, and (b) C_{SR}.

5.2. BER Performance. Next, we will use an optimized C_{SR} code profile $(\lambda(x), \rho(x))$ in Table 2 to analyze performance in terms of Bit Error Rate (BER) in the AWGN and Rayleigh fading channels, respectively. In simulations, the soft decision information from the demodulator is input into the decoder. The parameters used in simulations are listed in Table 3. The time partition parameter $t_1 = 0.7$ (obtained as in Section 5.2) is chosen to maximize the network coding capacity of the DF MARC model. Codeword length is 10^4.

In a *decode-and-forward* cooperative strategy, R needs to decode information from sources correctly. This requires the entire codeword to be correctly transmitted. Therefore, codes should have excellent frame error ratios (FERs). To ensure the FER performance of LDPC codes, small circles in the parity-check matrix must be removed. Then, parity-check matrices of C_{SR}, $C_{S_1}^{t_1}$, and $C_{S_2}^{t_1}$ are randomly constructed by $\lambda(x)$ and $\rho(x)$), respectively. Accordingly, the girth of length 4 in the bipartite graph has been detected and removed.

Figure 10 shows the BER curve against the SNR at the different $C_{S_1}^{t_1}$ (or $C_{S_2}^{t_1}$) code rate. Obviously, with the help of the cooperative mechanism, the result has a great improvement of performance on BER, because R is near to D and provides almost a 1.2 dB increase in spatial diversity in low SNR in the AWGN channel at a $C_{S_1}^{t_1}$ (or $C_{S_2}^{t_1}$) rate of 0.5. In the AWGN channel at a $C_{S_1}^{t_1}$ (or $C_{S_2}^{t_1}$) rate of 2/3, the performance still improves by 1 dB. In such

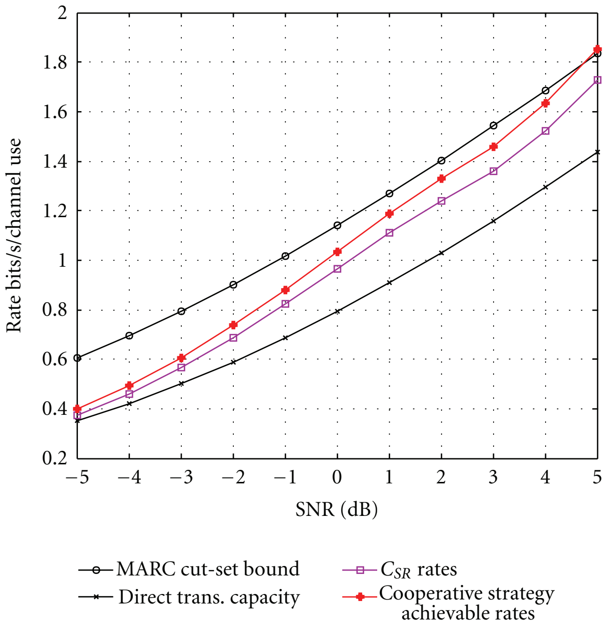

Figure 9: Achievable rates and capacity comparisons.

Table 3: Parameters in simulation.

Time partition	$t_1 = 0.7$
Codeword length	$N_S = 10^4$
Distance between S and R	Distance = 0.5
Channel model	AWGN, Rayleigh Fasting Fading and Rayleigh Slow Fading
Power	$E[x^2] = 0$ dBw
Max iteration	100
Modulation	BPSK, QPSK
Decoding algorithm	BP

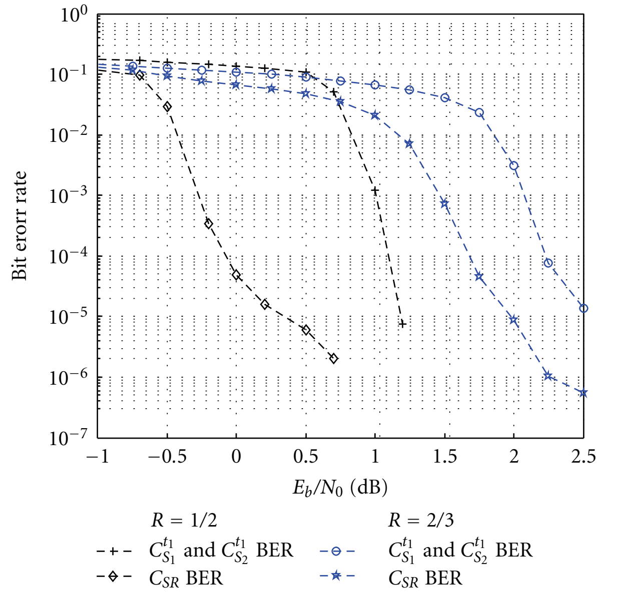

Figure 10: The BER performance under the AWGN channel with BPSK, $d = 0.5$.

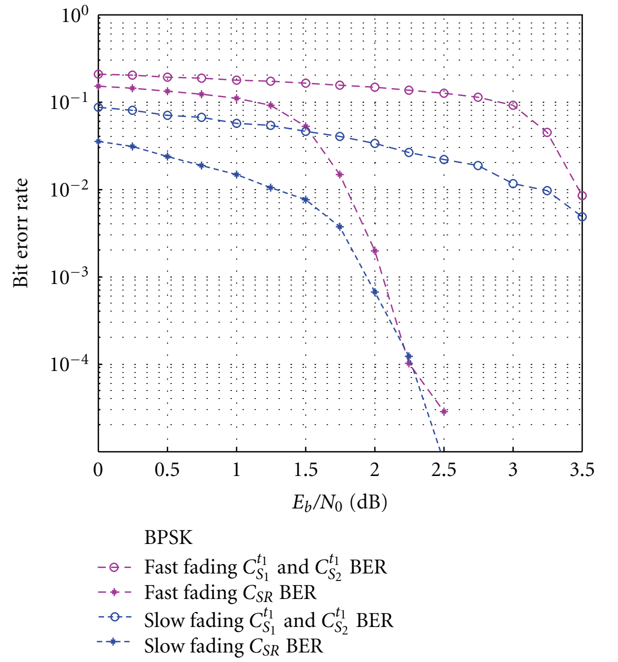

Figure 11: The BER performance under the Rayleigh Fading channel with BPSK, $d = 0.5$, and $R_{S_1R}^{t_1} = R_{S_2R}^{t_1} = 0.5$.

circumstances, the direct link between S and D cannot offer a service-satisfied physical layer QoS transmission, but with the cooperative relaying, the transmission will be employed again. The simulations demonstrate that this cooperative strategy has improved reliability, especially for the cases in low SNR.

In the Rayleigh channel as shown in Figures 11 and 12, the average gain in diversity is larger than 2 dB. Two kinds of modulation schemes are plotted to compare the performance: BPSK and QPSK. The BPSK scheme is shown to have a lower BER performance than the QPSK. Besides, the presented network-coded cooperative strategy has better BER performance under fast fading channel than that under slow fading channel. And it is concluded that in fast fading or mobile environment, the employment of a relay node indeed could provide effective spatial diversity.

We also intend to investigate the effects of the relay position factor d on BER performance. BER curves with $d = 0.1, 0.25$, $d = 0.35$, $d = 0.5$, $d = 0.6$, and $d = 0.8$ are plotted in Figure 13. The comparisons show that increasing d increases the performance of BER versus SNR. This is because the path loss of the RD channel decreases, which is easier to decode $C_R^{t_2}$, resulting in decoding of the extra check bits with a lower error rate. However, from Figure 5 in Section 3.1, when $d = 0.5$, the achievable sum-rate is optimal; the slope of the curve with $d > 0.5$ is larger than that of the curve with $d < 0.5$. In other words, as $d = 0.8$,

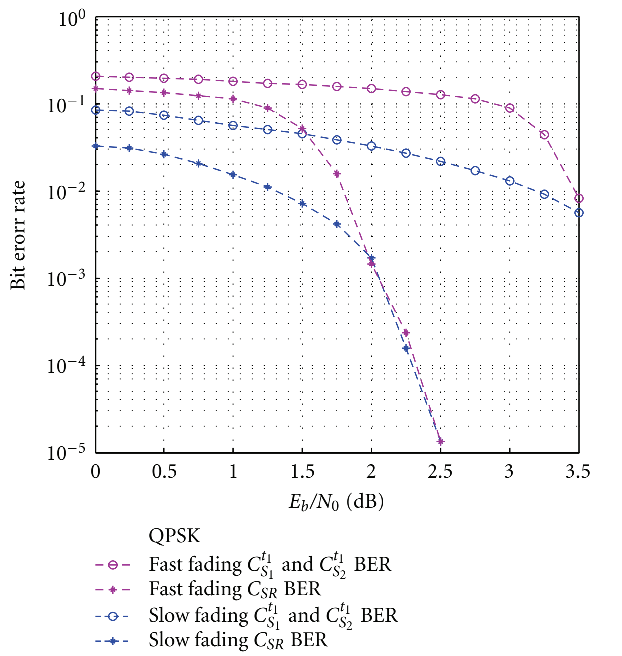

Figure 12: The BER performance under the Rayleigh Fading channel with QPSK, $d = 0.5$, and $R_{S_1R}^{t_1} = R_{S_2R}^{t_1} = 0.5$.

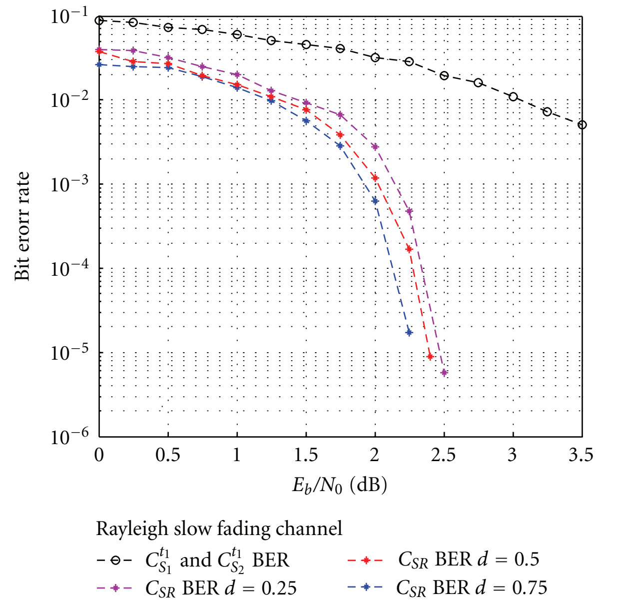

Figure 14: The BER performance under the Rayleigh Slow Fading channel with different settings of d, the distance between Source and Relay.

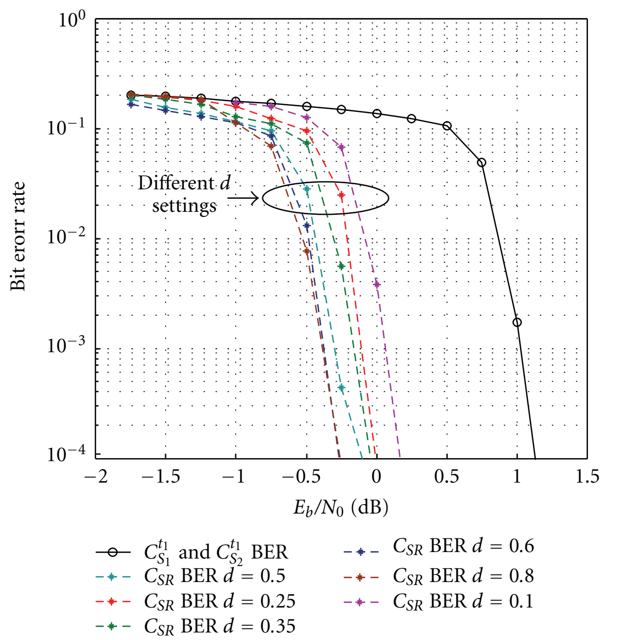

Figure 13: The BER performance under the AWGN channel with different settings of d, the distance between Source and Relay.

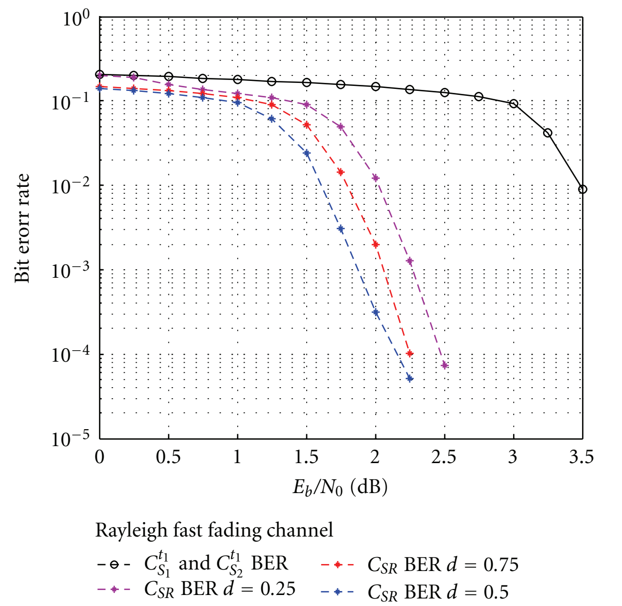

Figure 15: The BER performance under the Rayleigh Fast Fading channel with different settings of d, the distance between Source and Relay.

the achievable sum-rate is less than that as $d = 0.2$. Likewise, we also give the BER performance with different settings of the relay position factor d under Rayleigh Slow Fading and Rayleigh Fast Fading channels in Figure 14 and Figure 15. As a result, the spatial diversity and multiplexing can be balanced by the factor d in the parity-check network coding cooperative strategy.

Besides, we also investigate the effects of BER with different numbers of extra check bits under AWGN and Rayleigh Fading channels through Figure 16 to Figure 18. It is valid that the more extra bits are sent, the better the BER performances are, since the rate of cooperative code C_{SR} is reduced. Thereby, the spatial gain obtained by sending more extra check bits is at the cost of throughput of the whole

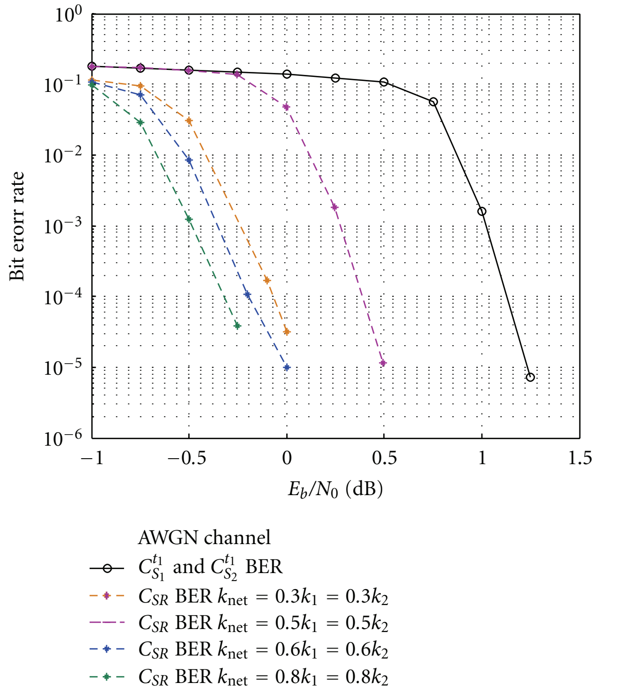

Figure 16: The BER performance under the AWGN channel with different lengths of extra check bits.

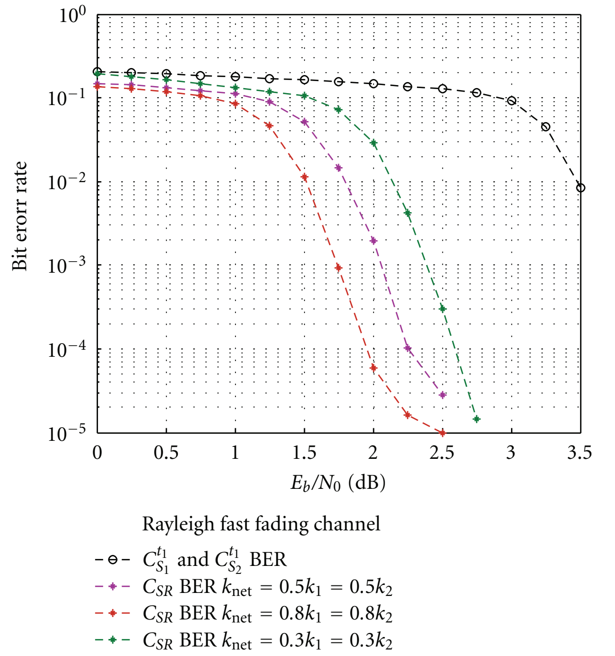

Figure 18: The BER performance under the Rayleigh Fast Fading channel with different lengths of extra check bits.

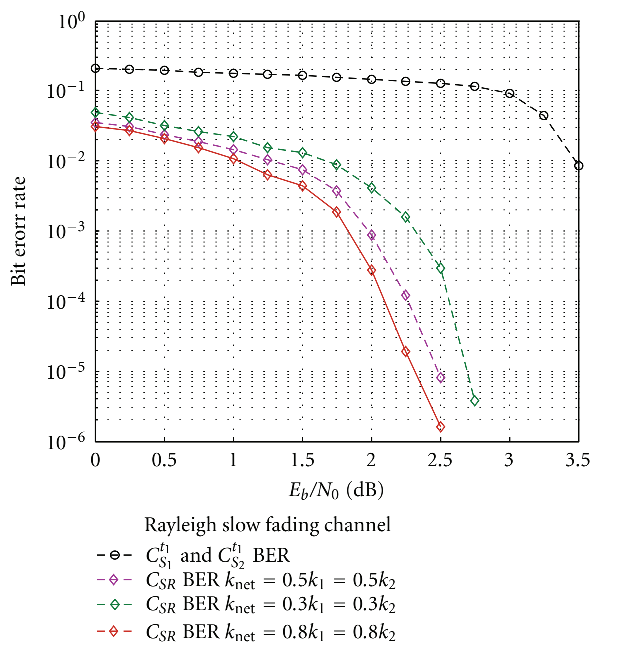

Figure 17: The BER performance under the Rayleigh Slow Fading channel with different lengths of extra check bits.

system. As a result, the spatial diversity and multiplexing can be balanced by maximizing the rate of the cooperative strategy to obtain optimal relay position d and optimal extra check bits length.

6. Conclusion

This study investigated a cooperative strategy based on parity-check network coding. The relative performance improvement of the schemes lies in a *decode-and-forward* strategy at the relay node. In particular, this study has revealed that a successful design should (1) employ the most effective extra check bits to make full use of the information contained in x_3 to help decode the messages from S_1 and S_2 and (2) perform linear network coding with the extra check bits. Specifically, we provide an implementation of parity-check network coding based on layered multidimensional LDPC code and a corresponding belief propagation decoding algorithm. The parity-check network coding for both sources removes the bandwidth loss that occurs in relaying, which is only 0.5 dB from the MARC DF "Cut-Set" capacity, and yet the parity-check bits ensures an attractive spatial diversity of cooperative communication. In the future, we would like to extend the proposed scheme to correlated multiple source nodes and conduct further research on network coding in GF(q) fields.

Appendix

Proof of Theorem 1. Rearrange the columns of the C_{SR} parity-check matrix according to the descending sequence of variable node degrees, such as $\{d_{v,SR}, d_{v,SR} - 1, \ldots, 3, 2\}$, and then successively deal with the numbers of variable nodes in each degree. The variable nodes in C_{SR} have two types of degrees, $\lambda_{i,j}^{SR}$, sub-LDPC degree i, $i \geq 2$ and extra degree j, $j \geq 0$. Therefore, the number of variable nodes with a specific degree d in C_{SR}, denoted by $N_d = (\lambda_d/d) \cdot E$, also has two parts: $N_{d,j=0}$, the number of degree d without extra checks in $C_{S_1}^{t_1}$ (or $C_{S_2}^{t_1}$); $N_{i<d,j\neq 0,i+j=d}$, the number of turning into degree d after extra checks added in $C_{S_1}^{t_1}$ (or $C_{S_2}^{t_1}$).

For the maximum degree $d_{v,SR}$ in cooperative C_{SR}, let $d_{v,S} = \max(d_{v,S_1}, d_{v,S_2})$ and $d_{v,SR} \geq d_{v,S}$. $N_{d_{v,S},j=0}$ represents the number of variable nodes in $C_{S_1}^{t_1}$ (or $C_{S_2}^{t_1}$). Clearly, for the maximum degree $d_{v,SR}$,

$$N_{d_{v,SR}} = N_{d_{v,S},j=0} + N_{\substack{i<d_{v,S},j\neq 0 \\ i+j=d_{v,S}}}. \tag{A.1}$$

Hence, $N_{d_{v,SR}} \geq N_{d_{v,S},j=0}$ is tenable, and based on $N_d = (\lambda_d/d)\cdot E$, we have

$$\frac{\lambda_{d_{v,SR}}}{d_{v,SR}} E_{SR} \geq \left(\frac{\gamma_{d_{v,S}}}{d_{v,S}} E_{S_1} + \frac{\gamma_{d_{v,S}}}{d_{v,S}} E_{S_2}\right). \tag{A.2}$$

If $d_{v,\mathrm{SR}} = \max(d_{v,S_1}, d_{v,S_2})$, then $\gamma_{d_{v,S}} \neq 0$; if $d_{v,SR} > \max(d_{v,S_1}, d_{v,S_2})$, then $\gamma_{d_{v,S}} = 0$.

Next, considering degree $d_{v,SR}-1$, the number of variable nodes with degrees larger than $d_{v,SR}-1$ is

$$\begin{aligned} &N_{d_{v,SR}} + N_{d_{v,SR}-1} \\ &\quad = \left(N_{d_{v,S},j=0} + N_{d_{v,S}-1,j=0}\right) + N_{\substack{i<(d_{v,S}-1),j\neq 0 \\ i+j=d_{v,S},(d_{v,S}-1)}}, \end{aligned} \tag{A.3}$$

where $(N_{d_{v,S},j=0} + N_{d_{v,S}-1,j=0})$ is the number of variable nodes with degrees larger than $d_{v,SR}-1$ in $C_{S_1}^{t_1}$ (or $C_{S_2}^{t_1}$). Thus, based on $N_d = (\lambda_d/d)\cdot E$, we obtain

$$\begin{aligned} &\left(\frac{\lambda_{d_{v,SR}}}{d_{v,SR}} + \frac{\lambda_{d_{v,SR}-1}}{d_{v,SR}-1}\right) E_{SR} \\ &\quad \geq \sum_{i=d_{v,SR},d_{v,SR}-1} \left(\frac{\gamma_{i,S_1}}{i} E_{S_1} + \frac{\gamma_{i,S_2}}{i} E_{S_2}\right). \end{aligned} \tag{A.4}$$

Then, for all degrees in the descending sequence in C_{SR}, it is confirmed that

$$\begin{aligned} &\left(N_{d_{v,SR}} + N_{d_{v,SR}-1} + \cdots + N_2\right) \\ &= \begin{pmatrix} \left(N_{d_{v,S},j=0} + N_{d_{v,S}-1,j=0} + \cdots + N_{2,j=0}\right) \\ +\left(N_{\substack{i<(d_{v,S}-1),j\neq 0 \\ i+j=d_{v,S},(d_{v,S}-1)}}\right) + \left(N_{\substack{i<(d_{v,S}-2),j\neq 0 \\ i+j=d_{v,S},(d_{v,S}-1),(d_{v,S}-2)}}\right) \\ + \cdots + \left(N_{\substack{i=2,j\neq 0 \\ i+j=d_{v,S},(d_{v,S}-1),\ldots,3}}\right) \end{pmatrix}. \end{aligned} \tag{A.5}$$

Using the expression in terms of degree distribution $N_d = (\lambda_d/d)\cdot E_{SR}$ to replace N_d, we have

$$\begin{aligned} \sum_{i=j}^{d_{v,SR}} \frac{\left(\lambda_{i,j}^{SR}\right)}{i} E_{SR} \geq \sum_{i=j}^{\max(d_{v,S_1},d_{v,S_2})} \left(\frac{\gamma_i^{S_1}}{i} E_{S_1} + \frac{\gamma_i^{S_2}}{i} E_{S_2}\right) \\ \forall j = 2, 3, \ldots, d_{v,SR}. \end{aligned} \tag{A.6}$$

Therefore, the relationships of (13) hold under the cooperative constructions. □

Acknowledgments

This work is supported by the National Nature Science Foundation of China (no. 60532030) and National Outstanding Youth Science Fund (no. 60625102).

References

[1] L. Sankaranarayanan, G. Kramer, and N. B. Mandayam, "Hierarchical sensor networks: capacity bounds and cooperative strategies using the multiple-access relay channel model," in *Proceedings of 1st Annual IEEE Communications Society Conference on Sensor and Ad Hoc Communications and Networks (SECON '04)*, pp. 191–199, October 2004.

[2] G. Kramer, M. Gastpar, and P. Gupta, "Cooperative strategies and capacity theorems for relay networks," *IEEE Transactions on Information Theory*, vol. 51, no. 9, pp. 3037–3063, 2005.

[3] A. Nosratinia, T. E. Hunter, and A. Hedayat, "Cooperative communication in wireless networks," *IEEE Communications Magazine*, vol. 42, no. 10, pp. 74–80, 2004.

[4] A. Sendonaris, E. Erkip, and B. Aazhang, "User cooperation diversity—part I: system description," *IEEE Transactions on Communications*, vol. 51, no. 11, pp. 1927–1938, 2003.

[5] J. N. Laneman, D. N. C. Tse, and G. W. Wornell, "Cooperative diversity in wireless networks: efficient protocols and outage behavior," *IEEE Transactions on Information Theory*, vol. 50, no. 12, pp. 3062–3080, 2004.

[6] J. N. Laneman and G. W. Wornell, "Distributed space-time-coded protocols for exploiting cooperative diversity in wireless networks," *IEEE Transactions on Information Theory*, vol. 49, no. 10, pp. 2415–2425, 2003.

[7] T. E. Hunter and A. Nosratinia, "Cooperation diversity through coding," in *Proceedings of IEEE International Symposium on Information Theory*, p. 220, July 2002.

[8] A. Chakrabarti, A. de Baynast, A. Sabharwal, and B. Aazhang, "Low density parity check codes for the relay channel," *IEEE Journal on Selected Areas in Communications*, vol. 25, no. 2, pp. 280–290, 2007.

[9] P. Razaghi and W. Yu, "Bilayer LDPC codes for the relay channel," in *Proceedings of IEEE International Conference on Communications (ICC '06)*, pp. 1574–1579, Istanbul, Turkey, July 2006.

[10] M. A. Khojastepour, *Distributed cooperative communications in wireless networks*, Ph.D. thesis, Rice University, Houston, Tex, USA , 2004.

[11] R. Ahlswede, N. Cai, S.-Y. R. Li, and R. W. Yeung, "Network information flow," *IEEE Transactions on Information Theory*, vol. 46, no. 4, pp. 1204–1216, 2000.

[12] E. C. van der Meulen, "Three- terminal communication channels," *Advances in Applied Probability*, vol. 3, no. 1, pp. 120–154, 1971.

[13] T. M. Cover and A. A. EL Gamal, "Capacity theorems for the relay channel," *IEEE Transactions on Information Theory*, vol. 25, no. 5, pp. 572–584, 1979.

[14] R. C. King, *Multiple access channels with generalized feedback*, Ph.D. thesis, Stanford University, Stanford, Calif, USA, 1978.

[15] S. Zhang, S. C. Liew, and P. P. Lam, "Hot topic: physical-layer network coding," in *Proceedings of the 12th Annual International Conference on Mobile Computing and Networking(MOBICOM '06)*, pp. 358–365, September 2006.

[16] S. Katti, S. Gollakota, and D. Katabi, "Embracing wireless interference: analog network coding," in *Proceedings of Conference on Computer Communications (SIGCOMM '07)*, pp. 397–408, August 2007.

[17] C. Hausl, F. Schreckenbach, I. Oikonomidis, and G. Bauch, "Iterative network and channel decoding on a tanner graph," in *Proceedings of the 43rd Annual Allerton Conference on Communications, Control, and Computing (GLOBECOM '05)*, Monticello, Va, USA, September 2005.

[18] X. Bao and J. Li, "Matching code-on-graph with networks-on-graph: adaptive network coding for wireless relay networks," in *Proceedings of the 43rd Annual Allerton Conference on Communications, Control, and Computing (GLOBECOM '05)*, Monticello, Ill, USA, September 2005.

[19] M. Effros, M. Medard, T. Ho, S. Ray, D. R. Karger, and R. Koetter, "Linear network codes: a unified framework for source, channel and network coding," in *Proceedings of DIMACS Workshop on Network Information Theory*, p. 179, Piscataway, NJ, USA, March 2003.

[20] Y. Chen, S. Kishore, and J. Li, "Wireless diversity through network coding," in *Proceedings of IEEE Wireless Communications and Networking Conference (WCNC '06)*, pp. 1681–1686, April 2006.

[21] L. Xiao, T. E. Fuja, J. Kliewer, and D. J. Costello Jr., "A network coding approach to cooperative diversity," *IEEE Transactions on Information Theory*, vol. 53, no. 10, pp. 3714–3722, 2007.

[22] S. Yang and R. Koetter, "Network coding over a noisy relay : a belief propagation approach," in *IEEE International Symposium on Information Theory (ISIT '07)*, pp. 801–804, Nice, France, June 2007.

[23] R. W. Yeung, S.-Y. R. Li, N. Cai, and Z. Zhang, "Network coding theory," *Foundations and Trends in Communications and Information Theory*, vol. 2, no. 4, pp. 241–329, 2006.

[24] M. A. Khojastepour, A. Sabharwal, and B. Aazhang, "On the capacity of 'cheap' relay networks," in *Proceedings of the 37th Annual Conference on Information Sciences and Systems*, Baltimore, Md, USA, March 2003.

[25] D. Slepian and J. K. Wolf, "Noiseless coding of correlated information sources," *IEEE Transactions on Information Theory*, vol. 19, no. 4, pp. 471–480, 1973.

[26] A. D. Wyner and J. Ziv, "The rate-distortion function for source coding with side information at the decoder," *IEEE Transactions on Information Theory*, vol. 22, no. 1, pp. 1–10, 1976.

[27] E. Sharon, A. Ashikhmin, and S. Litsyn, "Analysis of low-density parity-check codes based on EXIT functions," *IEEE Transactions on Communications*, vol. 54, no. 8, pp. 1407–1414, 2006.

[28] S.-Y. Chung, T. J. Richardson, and R. L. Urbanke, "Analysis of sum-product decoding of low-density parity-check codes using a Gaussian approximation," *IEEE Transactions on Information Theory*, vol. 47, no. 2, pp. 657–670, 2001.